available at www.sciencedirect.com

ScienceDirect

journal homepage: www.elsevier.com/locate/biochempharm

Cholesterol-lowering effect of bezafibrate is independent of peroxisome proliferator-activated receptor activation in mice

Takero Nakajima [a], *Naoki Tanaka* [a,b,*], *Eiko Sugiyama* [a,c], *Yuji Kamijo* [a,b], *Atsushi Hara* [a], *Rui Hu* [a,d], *Gang Li* [a,e], *Yufeng Li* [a], *Kozo Nakamura* [f], *Frank J. Gonzalez* [g], *Toshifumi Aoyama* [a]

[a] *Department of Metabolic Regulation, Institute on Aging and Adaptation, Shinshu University Graduate School of Medicine, Matsumoto, Japan*
[b] *Department of Internal Medicine, Shinshu University School of Medicine, Matsumoto, Japan*
[c] *Department of Nutritional Science, Nagano Prefectural College, Nagano, Japan*
[d] *The Second Hospital of Hebei Medical University, Shijiazhuang, Hebei, China*
[e] *Cardiac Center of Hebei Provincial People's Hospital, Shijiazhuang, Hebei, China*
[f] *Department of Bioscience and Biotechnology, Faculty of Agriculture, Shinshu University, Nagano, Japan*
[g] *Laboratory of Metabolism, National Cancer Institute, Bethesda, MD, USA*

ARTICLE INFO

Article history:
Received 11 February 2008
Accepted 2 April 2008

Keywords:
Bezafibrate
Peroxisome proliferator-activated receptor (PPAR)
Ppara-null mice
Cholesterol metabolism
Sterol regulatory element-binding protein (SREBP) 2

ABSTRACT

The hypocholesterolemic potential of peroxisome proliferator-activated receptor (PPAR) pan-activator bezafibrate has been documented. However, in addition to uncertainty about the contribution of PPARα to its effect, there is a marked discrepancy in bezafibrate dosages used in previous rodent experiments (≥50 mg/kg/day) and those in clinical use (≤10 mg/kg/day). To investigate the association between bezafibrate-induced cholesterol reduction and PPARα activation, wild-type and *Ppara*-null mice were treated with bezafibrate at high (100 mg/kg/day) or low (10 mg/kg/day) doses and analyzed. High-dose treatment decreased hepatic cholesterol content in wild-type mice, but increased serum cholesterol concentration. In liver samples, simultaneous increases in the expression of numerous proteins involved in cholesterol biosynthesis and catabolism, as well as cholesterol influx and efflux, were observed, which made interpretation of phenotype changes subtle. These complicated responses were believed to be associated with intensive PPAR activation and accompanying up-regulation of liver X receptor α, farnesoid X receptor, and sterol regulatory element-binding protein 2 (SREBP2). In contrast, low-dose bezafibrate treatment decreased serum and hepatic cholesterol concentrations in a PPARα-independent manner, probably from

* *Corresponding author at*: Department of Metabolic Regulation, Institute on Aging and Adaptation, Shinshu University Graduate School of Medicine, 3-1-1 Asahi, Matsumoto 390-8621, Japan. Tel.: +81 263 37 2850; fax: +81 263 37 3094.
E-mail address: naopi@hsp.md.shinshu-u.ac.jp (N. Tanaka).

Abbreviations: ABC, ATP-binding cassette; ABCA1, ABC transporter A1; ACAT2, acyl-CoA:cholesterol acyltransferase 2; ACC2, acetyl-CoA carboxylase 2; AOX, acyl-CoA oxidase; AOX2, branched-chain AOX; aP2, adipocyte fatty acid-binding protein; apo, apolipoprotein; AUC, area under the concentration–time curve; BAAT, bile acid-CoA:amino acid *N*-acyltransferase; BSEP, bile salt export pump; CD36, fatty acid translocase; Ch25h, cholesterol 25-hydroxylase; C_{max}, maximum plasma concentrations; CTE, cytosolic thioesterase; CYP7A1, cholesterol 7α-hydroxylase; CYP27A1, sterol 27-hydroxylase; CYP7B1, oxysterol 7α-hydroxylase; CYP8B1, sterol 12α-hydroxylase; DAB, 3,3′-diaminobenzidine; FPPS, farnesyl pyrophosphate synthase; FXR, farnesoid X receptor; GAPDH, glyceraldehyde-3-phosphate dehydrogenase; HMGR, 3-hydroxy-3-methylglutaryl-CoA reductase; HMGS, 3-hydroxy-3-methylglutaryl-CoA synthase; 3β-HSD, 3β-hydroxysteroid dehydrogenase; LDLR, low-density lipoprotein receptor; L-FABP, liver fatty acid-binding protein; LXR, liver X receptor; Mdr, multidrug resistance; Mrp, multidrug resistance-associated protein; NPC1, Niemann-Pick type C1 protein; NTCP, sodium-taurocholate cotransporting polypeptide; OATP, organic anion transporting polypeptide; PCR, polymerase chain reaction; PDK4, pyruvate dehydrogenase kinase 4; PPAR, peroxisome proliferator-activated receptor; SCP2, sterol carrier protein 2; SQS, squalene synthase; SR-B1, scavenger receptor B1; SREBP, sterol regulatory element-binding protein; TC, total cholesterol.

0006-2952/$ – see front matter
doi:10.1016/j.bcp.2008.04.001

suppression of SREBP2-regulated cholesterogenesis and enhancement of cholesterol catabolism due to elevated 7α-hydroxylase levels. Interestingly, the low-dose treatment did not affect the expression of PPAR target genes or number of peroxisomes, suggesting the absence of PPAR activation. These results demonstrate that the action of bezafibrate on cholesterol metabolism may vary with dosage, and that the cholesterol-reducing effect found in mice at dosages similar to those administered to humans is independent of significant PPAR activation.

1. Introduction

Bezafibrate, a second-generation fibrate drug, is used clinically as a hypolipidemic agent. Bezafibrate treatment lowers serum triglyceride and cholesterol levels by more than 25% and 10%, respectively, in patients with hyperlipidemia [1–4], and the Bezafibrate Infarction Prevention study has demonstrated a relationship between the lipid-lowering effects of bezafibrate and a reduction of the risk of cardiovascular events in dyslipidemic patients with coronary artery disease [5]. The molecular mechanism underlying the triglyceride-reducing effect of bezafibrate is due in part to the induction of lipoprotein lipase activity mediated by the activation of peroxisome proliferator-activated receptor α (PPARα), a member of the nuclear receptor superfamily [6,7]. However, the molecular mechanism underlying its effect on cholesterol metabolism has not yet been fully elucidated.

PPARα is highly expressed in the liver, kidney, and heart, and functions as a critical regulator of fatty acid metabolism [8–11]. Recently, several studies using a *Ppara*-null mouse model established a possible direct involvement of PPARα in the regulation of cholesterol metabolism. For example, PPARα activation enhances hepatic expression of mRNA encoding sterol 12α-hydroxylase (CYP8B1), an enzyme involved in bile acid synthesis from cholesterol [12], and multidrug resistance 2 (Mdr2), a phospholipid transporter for bile formation [13]. On the other hand, it is known that bezafibrate can also activate other PPAR subtypes [β (δ) and γ] [14–16]. Thus, it remains unclear whether the effect of bezafibrate on cholesterol reduction is singularly due to its effect on PPARα.

In the present study, the contribution of PPARα to the cholesterol-reducing effect of bezafibrate was examined using *Ppara*-null mice. With respect to this issue, there is a marked discrepancy between bezafibrate dosages used in previous rodent studies and those typically administered in the clinic; although the appropriate dosage for humans is estimated to be less than or equal to 10 mg/kg/day, studies in rodent models have often opted for high-dose regimens (50 mg/kg/day or more) [16–19]. In the present study, therefore, wild-type and *Ppara*-null mice were treated with bezafibrate at high (100 mg/kg/day) or low (10 mg/kg/day) doses. Unexpectedly, low-dose bezafibrate treatment reduced serum and hepatic cholesterol concentrations in the absence of prominent PPAR activation.

2. Materials and methods

2.1. Materials

Bezafibrate (2-{4-[2-(4-chlorobenzamido)ethyl]phenoxy}-2-methylpropionic acid) was kindly provided by Kissei Pharmaceutical Co., Ltd. (Matsumoto, Japan). Carboxymethylcellulose, Cholesterol E-Test kit, Free Cholesterol E-Test kit, Triglyceride E-Test kit, and Triton X-100 were purchased from Wako Pure Chemical Industries, Ltd. (Osaka, Japan), and 3,3′-diaminobenzidine (DAB) tetrahydrochloride was from Dojindo Laboratories (Kumamoto, Japan). RNeasy Mini Kit was obtained from QIAGEN (Hilden, Germany). Reverse transcript reagents were purchased from Invitrogen Corporation (Carlsbad, CA, USA). Power SYBR Green PCR Master Mix was obtained from Applied Biosystems (Foster City, CA, USA). BCA Protein Assay Kit and 1-Step NBT/BCIP reagent were purchased from Pierce Biotechnology (Rockford, IL, USA). Nitrocellulose membrane was obtained from GE Healthcare (Little Chalfont, UK). Rabbit polyclonal antibodies against 3-hydroxy-3-methylglutaryl-CoA reductase (HMGR), cholesterol 7α-hydroxylase (CYP7A1), sterol regulatory element-binding protein 2 (SREBP2), fatty acid translocase (CD36), actin, and histone H1, as well as goat polyclonal antibodies against squalene synthase (SQS), oxysterol 7α-hydroxylase (CYP7B1), acetyl-CoA carboxylase 2 (ACC2), pyruvate dehydrogenase kinase 4 (PDK4), and adipocyte fatty acid-binding protein (aP2) were purchased from Santa Cruz Biotechnology (Santa Cruz, CA, USA). Rabbit polyclonal antibodies against acyl-CoA oxidase (AOX) and cytosolic thioesterase (CTE) were described elsewhere [20,21]. Alkaline phosphatase-conjugated goat anti-rabbit IgG and rabbit anti-goat IgG antibodies were obtained from Jackson ImmunoResearch Laboratories (West Grove, PA, USA).

2.2. Animals and bezafibrate treatment

Ppara-null mice on a Sv/129 genetic background were described elsewhere [22]. Twelve-week-old male Sv/129 wild-type and *Ppara*-null mice (25–30 g body weight) were assigned to one of three groups (control group, low-dose bezafibrate group, or high-dose bezafibrate group; $n = 6$ in each). The mice were housed in a temperature- and light-controlled environment (25 °C; 12 h light/dark cycle) and maintained with tap water *ad libitum* and a 7% fat-containing standard rodent diet. Bezafibrate was suspended in 1% (w/v) carboxymethylcellulose at final concentrations of 1.5 and 15 mg/mL for the 10 and 100 mg/kg/day treatments, respectively, and 0.2 mL of each suspension was administered by gavage once a day (10:00 a.m.) for 10 days. The same amount of 1% (w/v) carboxymethylcellulose without bezafibrate was administered in a similar manner to control mice. At the end of treatment, food was withdrawn from all mice overnight, mice were killed under anesthesia, and blood and livers were collected for analysis. All animal experiments were conducted in accordance with the animal care guidelines approved by the Shinshu University School of Medicine.

2.3. Measurement of lipids

Serum total cholesterol (TC) and triglyceride concentrations were measured using the Cholesterol E-Test and Triglyceride E-Test kits, respectively. Serum lipoprotein profiles were analyzed by high-performance liquid chromatography with an on-line dual detection system (Skylight Biotech., Akita, Japan) [23]. To measure hepatic cholesterol content, total lipid in liver tissue (50 mg) was extracted according to the hexane/isopropanol method [24]. The lipid extract was solubilized in distilled water by the addition of Triton X-100 as described previously with minor modifications [25], and cholesterol was then measured. Measurement of liver free cholesterol content was carried out using the Free Cholesterol E-Test kit. Liver cholesteryl ester levels were calculated as the difference between liver TC and free cholesterol levels.

2.4. Analysis of mRNA expression

Total liver RNA was extracted using the RNeasy Mini Kit, and mRNA was reverse-transcribed using oligo-dT priming. Levels of mRNA were determined by quantitative real-time polymerase chain reaction (PCR) using SYBR Green chemistry on an ABI PRISM 7000 sequence detection system (Applied Biosystems). Specific primers were designed by Primer Express software (Applied Biosystems; Table 1). Each mRNA level was normalized to glyceraldehyde-3-phosphate dehydrogenase (GAPDH) mRNA, and then normalized to that of control wild-type mice.

Table 1 – Primers used for real-time PCR

Gene	Forward primers (5′ → 3′)	Reverse primers (5′ → 3′)	NCBI GenBank
ABCA1	GCAAGGCCGCACCATTAT	GTAACCCGTTCCCAACTGGTTT	NM_013454
ABCG1	CCTGAACTACTGGTACAGCCTGAA	TGGGACGTCATCCAGTATACGA	NM_009593
ABCG5	AAATCAAATTGTCCTTCTCTTGGC	CCACAGAACACCAACTCTCCG	NM_031884
ABCG8	GCAAAGGAACTCAACACAAGCAC	TCCCGGAAGTCATTGGAAATC	NM_026180
ACAT2	TGCAATGGACTCGACATATGGA	CAACAGCTCTGCCAACTCTCTCT	AF078751
ACC2	CCTCGGGACCACCTATGTGTAC	TCCAACACCAGCTCTGTGTATGT	BC022940
AOX	TGGTATGGTGTCGTACTTGAATGAC	AATTTCTACCAATCTGGCTGCAC	NM_015729
AOX2	TGGTCCTAGCCCATTTGATCTG	GGGCCTATGTCCCCAACTG	BC021339
aP2	TTTCCTTCAAACTGGGCGTG	AGGGTTATGATGCTCTTCACCTTC	NM_024406
apoA1	TGTGGATGCGGTCAAAGACA	AGGAGATTCAGGTTCAGCTGTTG	NM_009692
apoA2	GAGCATGACTGAATATGGCAAAGA	TATGCCTTGACCTGGCTCTGA	NM_013474
apoE	TTCGAGCCAATAGTGGAAGACA	TGTTGTTGCAGGACAGGAGAAG	NM_009696
BAAT	ATGGAGTTCCGAGCCAGTCTT	GCAGGTCATCATAGTTCCAGTAAGC	U95215
BSEP	TCAGTTCCTCCGTTCAAACATTG	TCTCTTTGGTGTTGTCCCCATA	NM_021022
CD36	CCAAATGAAGATGAGCATAGGACAT	GTTGACCTGCAGTCGTTTTGC	NM_007643
Ch25h	ACCCACTCACCATCTTTACCTTTC	AGTGGACCACGGGAAGTCATAG	NM_009890
CTE	CAAAGCCCTCTGGTAGACAAGAA	TGACCTACGAGGAACAGGAAGGT	NM_012006
CYP7A1	CGCATGTTTCTCAACGACACA	ATGCCCAGAGGATCACAAGGT	NM_007824
CYP27A1	GCAACTGATGCTGTCAAGGC	CACAGTCTTTACTTCTCCCATCCC	NM_024264
CYP7B1	CGAGAAGTGCAGGAGGATATGA	GTGGAGGAAAGAGGGCTACAAA	NM_007825
CYP8B1	GGCTGGCTTCCTGAGCTTATT	CGGAACTTCCTGAACAGCTCAT	NM_010012
FPPS	ACATGGCAGGCATTGATGG	AAGAGATCAAGGTAGTCGTCCTGG	AF309508
FXR	GATTTGGAATCGTACTCCCCATAC	GAAGCCCAGGTTGGAATAGTAAGA	NM_009108
GAPDH	TGCACCACCAACTGCTTAG	GGATGCAGGGATGATGTTCTG	M32599
HMGR	TGTGGTTTGTGAAGCCGTCAT	CGTCAACCATAGCTTCCGTAGTT	M62766
HMGS	CAGGAAATGCCAGACCTACAGG	AGTCATAGGCATGCTGCATGTG	BC029603
3β-HSD	GGAGGCCTGTGTTCAAGCAA	GGCCCTGCAACATCAACTG	M58567
LDLR	GATGGACCAGGCCCCTAACT	GGTGTCAGCCACAGATACGCT	NM_010700
L-FABP	GCAGAGCCAGGAGAACTTTGAG	TTTGATTTTCTTCCCTTCATGCA	NM_017399
LXRα	GCGTCCATTCAGAGCAAGTGT	TCACTCGTGGACATCCCAGAT	AF085745
Mdr1	GCTATCACAGCCAGCATTTCG	CATTTGAGAGGACCAAGGATGTC	NM_011075
Mdr2	CGATACTCTGACTGGCAGGATAAA	ATCTGTCATTTCTCCAAAGACTATCATC	NM_008830
Mrp2	GCAAGTCCAACATGGCCTATTC	CGTAACGCTACTCAGAAATGAAGC	NM_013806
Mrp3	ATCCCTTTGGCCGATACTCG	GCCTCTGGCCAACACTGAGA	AY841885
NPC1	GCTCTTCTGGCCTGGTATTTGT	GGCCCAAAGTGCTTGTCAA	NM_008720
NTCP	TCTGGTAGTTATGTTGCTGCTCATC	AGTGAGCCTTGATCTTGCTGAAC	NM_011387
OATP1	CCCGCAGTCTTCATTCTAATCC	TGAGCTTCATCTCTGCAAGTTCAG	NM_013797
OATP2	TGCTGACTGCAACACAAAGTGTAG	GAGGCAAGCTGACATGTATGATAGAC	AB031814
PDK4	CACGTACTCCACTGCTCCAACA	TTGGCGTAGAGACGAGAAATTG	NM_013743
PPARα	CCTCAGGGTACCACTACGGAGT	GCCGAATAGTTCGCCGAA	NM_011144
PPARβ	TCAACATGGAATGTCGGGTG	ATACTCGAGCTTCATGCGGATT	NM_011145
PPARγ	TTCCACTATGGAGTTCATGCTTGT	TCCGGCAGTTAAGATCACACCTA	NM_011146
SCP2	CGGAGGAAAGTGGGTCATCA	GCACTGAGCCAGACCTGTTG	BC018384
SQS	CCGGAACCAGAGTGTGTTTAACT	CCTTCCGAATCTTCACTACTCCTT	NM_010191
SR-B1	CACCTTCAATGACAACGACACC	TCTCTGAGCCATGCGACTTG	NM_016741
SREBP2	GGTGTGATTGTCTTGAGCGTCTT	AGCTGCGAAATCACCTTTGG	XM_127995

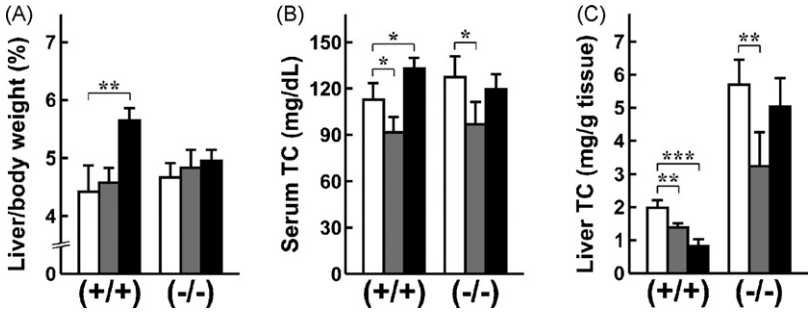

Fig. 1 – Phenotype changes by bezafibrate treatment in wild-type (+/+) and *Ppara*-null (−/−) mice. Liver/body weight ratio (A) and total cholesterol (TC) level in serum (B) and liver (C) were measured. Data are expressed as mean ± S.D. ($n = 6$ in each group). White bar, control group; gray bar, low-dose (10 mg/kg/day) bezafibrate group; black bar, high-dose (100 mg/kg/day) bezafibrate group. *P < 0.05, **P < 0.01, ***P < 0.001, between treated and untreated mice of the same genotype.

2.5. *Immunoblot analysis*

Preparations of whole liver lysate and hepatic nuclear fraction were performed as described previously [26–28]. Protein concentrations were determined using the BCA Protein Assay Kit. Whole liver lysates or nuclear fractions (50 μg protein) were subjected to sodium dodecyl sulfate-polyacrylamide gel electrophoresis and transferred to nitrocellulose membranes. After blocking, these membranes were incubated with primary antibodies followed by alkaline phosphatase-conjugated secondary antibodies, and then treated with 1-Step NBT/BCIP substrate. The position of protein bands was determined by molecular weight. Band intensity was quantified densitometrically, normalized to that of actin or histone H1, and then normalized to that of control wild-type mice.

2.6. *Cytochemical staining and morphometric analysis of hepatic peroxisomes*

Cytochemical staining of hepatic peroxisomes was carried out using the DAB technique as described elsewhere [28]. DAB-stained liver sections were visualized with both light and electron microscopy. Morphometric analysis of peroxisomes was also performed using electron micrographs at an original magnification of 4000×. For each mouse, 10 independent fields in the pericentral area of liver lobuli were photomicrographed, and the number of peroxisomes and area of each individual peroxisomal profile were measured. The numerical density and volume density of peroxisomes were calculated as follows: numerical density (number/μm^2) = $N_P/(A_T - A_{empty})$, and volume density (%) = $A_{TP}/(A_T - A_{empty}) \times 100$, where N_P was the peroxisome number in the test area, A_T was the test area, A_{empty} was the area composed of vascular and biliary lumens and hepatocyte nuclei, and A_{TP} was the area of total peroxisomal profiles in the test area. All areas were measured by a Luzex AP image analyzer (Nireco, Tokyo, Japan).

2.7. *Statistical analysis*

Results are expressed as mean ± S.D. Statistical analysis was performed using SPSS software 11.5J for Windows (SPSS inc., Chicago, IL, USA). Comparison between the groups was made by means of Student's *t*-test. A $P < 0.05$ was considered to be statistically significant.

3. Results

3.1. *Phenotype changes*

All mice appeared to be healthy during the experimental period, and no significant differences in food consumption or body weight were observed. Liver/body weight ratio was increased only in wild-type mice that received high-dose bezafibrate (Fig. 1A). Serum TC concentrations were slightly increased by high-dose bezafibrate treatment in wild-type, but not in *Ppara*-null mice, and were decreased by low-dose bezafibrate in both genotypes (Fig. 1B). Serum triglyceride concentrations were decreased in mice treated with low-dose bezafibrate compared with controls (94.1 ± 10.3 mg/dL vs. 123.5 ± 16.8 mg/dL in wild-type mice, $P = 0.037$; 71.6 ± 11.2 mg/dL vs. 94.6 ± 10.3 mg/dL in *Ppara*-null mice, $P = 0.033$). There was no pronounced alteration in lipoprotein composition from the treatment, since amounts of very-low-density lipoprotein and low-density lipoprotein were far less than those of high-density lipoprotein (data not shown). Liver TC content was significantly reduced by high-dose treatment in wild-type mice, and by low-dose treatment in both genotypes (Fig. 1C). Hepatic free cholesterol content was also decreased in mice treated with low-dose bezafibrate compared with controls (1.19 ± 0.06 mg/g vs. 1.47 ± 0.08 mg/g tissue in wild-type mice, $P = 0.004$; 1.79 ± 0.36 mg/g vs. 3.03 ± 0.45 mg/g tissue in *Ppara*-null mice, $P = 0.005$). The ratio of cholesteryl ester to TC was decreased in wild-type mice only (14.7 ± 3.2% vs. 25.9 ± 4.8%, $P = 0.008$). These two parameters were also reduced in wild-type mice that received high-dose bezafibrate (data not shown). These findings indicate that the cholesterol-lowering effect of bezafibrate occurs in a PPARα-independent manner in cases of low-dose administration.

3.2. *Effects on cholesterol biosynthesis*

To elucidate the molecular mechanism of the effects of bezafibrate, hepatic expression of mRNA encoding cholesterol biosynthetic enzymes was first measured. High-dose bezafibrate treatment markedly increased the expression of

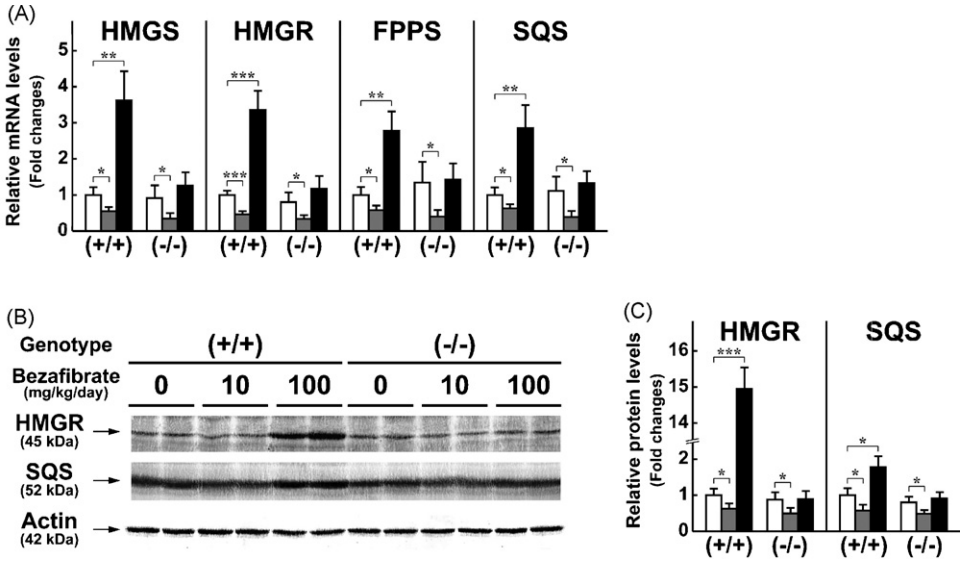

Fig. 2 – Effects of bezafibrate on cholesterol biosynthesis in wild-type (+/+) and *Ppara*-null (−/−) mice. (A) Hepatic expression of mRNA encoding cholesterol biosynthetic enzymes was analyzed by quantitative real-time PCR and normalized to that of GAPDH mRNA. Relative mRNA levels are shown as fold-changes of those of control wild-type mice. Data are expressed as mean ± S.D. (n = 6 in each group). White bar, control group; gray bar, low-dose (10 mg/kg/day) bezafibrate group; black bar, high-dose (100 mg/kg/day) bezafibrate group. *$P < 0.05$, **$P < 0.01$, ***$P < 0.001$, between treated and untreated mice of the same genotype. (B) Immunoblot analysis of HMGR and SQS. Fifty microgram of whole liver lysate protein was loaded into each well. The actin band was used as the loading control. Results are representative of three independent experiments. Doses of bezafibrate are indicated above the bands of each treatment group. (C) Quantification of HMGR and SQS protein levels. Band intensity was quantified densitometrically and normalized to that of actin. Relative protein levels are shown as fold-changes of those of control wild-type mice. Data are expressed as mean ± S.D. (n = 6 in each group). Bars are identical to those in panel A. *$P < 0.05$, ***$P < 0.001$, between treated and untreated mice of the same genotype.

3-hydroxy-3-methylglutaryl-CoA synthase (HMGS), HMGR, farnesyl pyrophosphate synthase (FPPS), and SQS mRNA in wild-type mice only (Fig. 2A), suggesting that these changes may be mediated by PPARα. In contrast, low-dose bezafibrate treatment significantly decreased the expression of HMGS, HMGR, FPPS, and SQS mRNA in both genotypes (Fig. 2A). Immunoblot analysis revealed that changes in HMGR and SQS protein expression were consistent with those in mRNA levels (Fig. 2B and C). These results demonstrate that de novo cholesterogenesis pathway is markedly suppressed specifically by low-dose bezafibrate treatment in both genotypes.

3.3. *Effects on cholesterol catabolism*

To determine whether bezafibrate treatment affected cholesterol catabolism, the expression of mRNA encoding bile acid synthetic enzymes was examined. High-dose bezafibrate treatment markedly increased the expression of CYP7A1, CYP8B1, and branched-chain AOX (AOX2) in wild-type mice, while their *Ppara*-null counterparts exhibited an increase in CYP7A1 expression, but a decrease in CYP8B1 (Fig. 3A). On the other hand, low-dose treatment significantly enhanced the expression of CYP7A1 and CYP7B1 mRNA in both genotypes (Fig. 3A). These increases were confirmed by immunoblot analysis (Fig. 3B and C). Bezafibrate treatment did not affect the expression of mRNA encoding sterol 27-hydroxylase (CYP27A1), 3β-hydroxysteroid dehydrogenase (3β-HSD), or cholesterol 25-hydroxylase (Ch25h). These results suggest that increased expression of two cholesterol-catabolizing enzymes (i.e., CYP7A1 and CYP7B1) may at least partially contribute to the cholesterol-reducing effect observed in wild-type and *Ppara*-null mice administered with low-dose bezafibrate.

3.4. *Effects on cholesterol influx, efflux, and intracellular sterol transport*

Next, the expression of mRNA encoding proteins involved in cholesterol influx and efflux was investigated. In wild-type mice, high-dose bezafibrate treatment markedly enhanced the expression of apolipoprotein A2 (apoA2), apoE, ATP-binding cassette (ABC) transporter A1 (ABCA1), scavenger receptor B1 (SR-B1), and low-density lipoprotein receptor (LDLR) mRNA, while low-dose treatment increased that of ABCA1 (Fig. 4A and B). These changes were not observed in similarly treated *Ppara*-null mice.

The expression of mRNA encoding sterol transporters and acyltransferases was also evaluated to determine the effect of bezafibrate on the intracellular mobility of cholesterol and its metabolites. High-dose bezafibrate treatment significantly elevated mRNA levels of Niemann-Pick type C1 protein (NPC1), sterol carrier protein 2 (SCP2), liver fatty acid-binding protein (L-FABP), and acyl-CoA:cholesterol acyltransferase 2 (ACAT2) in wild-type mice (Fig. 4C and D). *Ppara*-null mice that received high-dose bezafibrate showed an increase in L-FABP

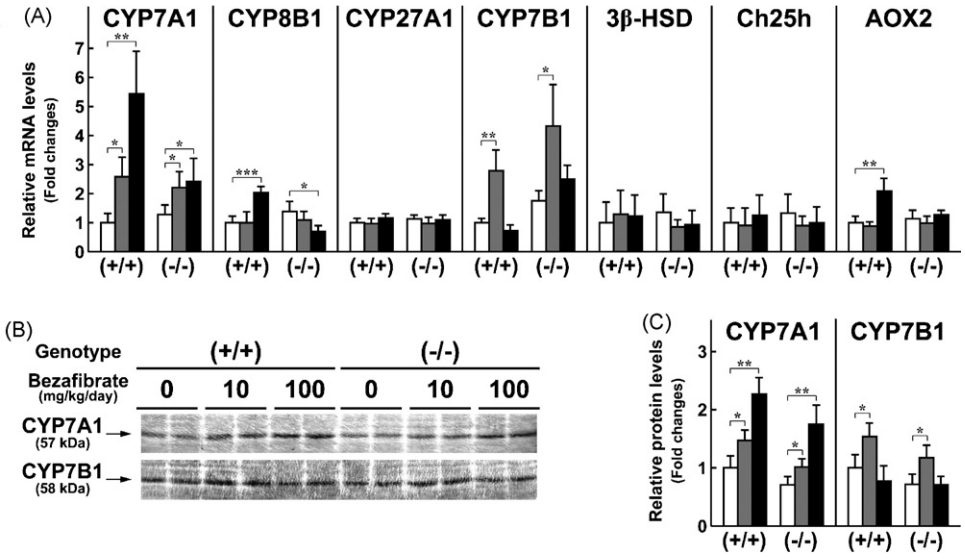

Fig. 3 – Effects of bezafibrate on cholesterol catabolism in wild-type (+/+) and *Ppara*-null (−/−) mice. (A) Hepatic expression of mRNA encoding cholesterol-catabolizing enzymes was analyzed by quantitative real-time PCR and normalized to that of GAPDH mRNA. Relative mRNA levels are shown as fold-changes of those of control wild-type mice. Data are expressed as mean ± S.D. (n = 6 in each group). Bars are identical to those in Fig. 2A. *P < 0.05, **P < 0.01, ***P < 0.001, between treated and untreated mice of the same genotype. (B) Immunoblot analysis of CYP7A1 and CYP7B1. The same samples in Fig. 2B were used. Protein sample of 50 μg was loaded into each well. (C) Quantification of CYP7A1 and CYP7B1 protein levels. Band intensity was quantified densitometrically and normalized to that of actin. Relative protein levels are shown as fold-changes of those of control wild-type mice. Data are expressed as mean ± S.D. (n = 6 in each group). Bars are identical to those in Fig. 2A. *P < 0.05, **P < 0.01, between treated and untreated mice of the same genotype.

mRNA expression. Low-dose bezafibrate treatment also elevated mRNA levels of NPC1 and L-FABP in wild-type mice, but not in *Ppara*-null mice (Fig. 4C and D). Bile acid-CoA:amino acid *N*-acyltransferase (BAAT) mRNA expression was unchanged.

3.5. *Effects on bile secretion and bile acid reabsorption*

High-dose bezafibrate treatment markedly increased mRNA expression of transporters related to bile secretion, including Mdr1, Mdr2, multidrug resistance-associated protein 2 (Mrp2),

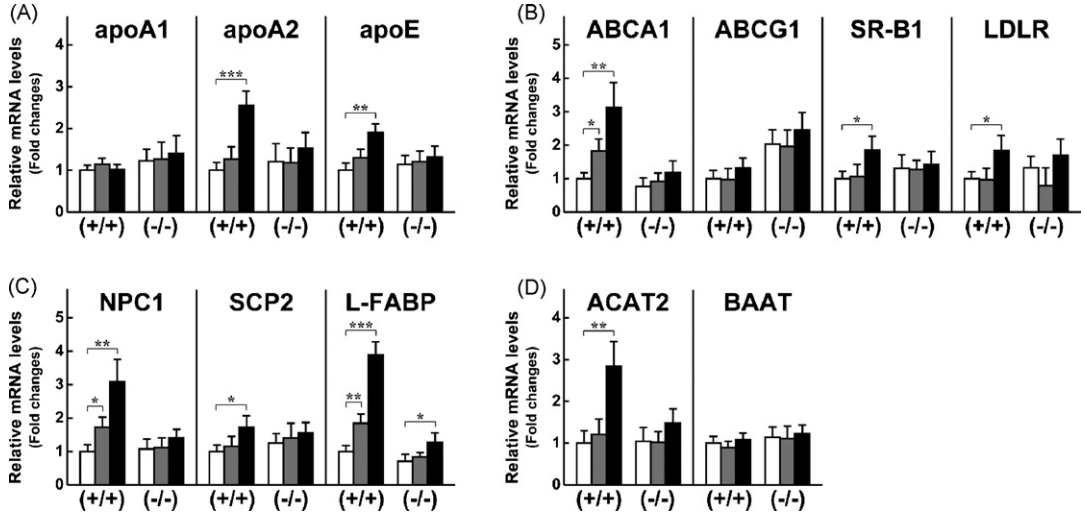

Fig. 4 – Effects of bezafibrate on cholesterol influx, efflux, and intracellular sterol transport in wild-type (+/+) and *Ppara*-null (−/−) mice. Hepatic expression of mRNA encoding apolipoproteins (A), cholesterol transporters and receptors (B), intracellular sterol transporters (C), and acyltransferases (D) was analyzed by quantitative real-time PCR and normalized to that of GAPDH mRNA. Relative mRNA levels are shown as fold-changes of those of control wild-type mice. Data are expressed as mean ± S.D. (n = 6 in each group). Bars are identical to those in Fig. 2A. *P < 0.05, **P < 0.01, ***P < 0.001, between treated and untreated mice of the same genotype.

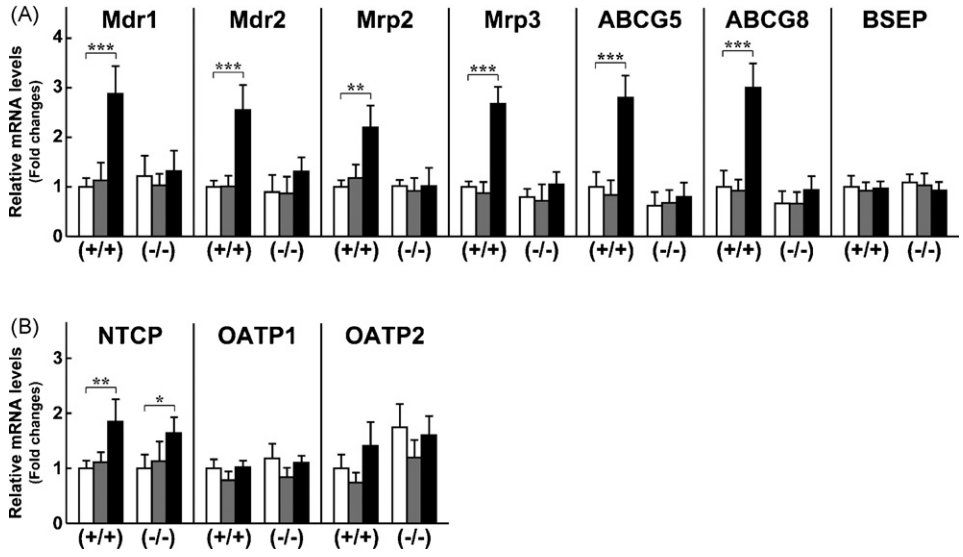

Fig. 5 – Effects of bezafibrate on bile secretion and bile acid reabsorption in wild-type (+/+) and *Ppara*-null (−/−) mice. Hepatic expression of mRNA encoding transporters related to bile secretion (A) and bile acid reabsorption (B) was analyzed by quantitative real-time PCR and normalized to that of GAPDH mRNA. Relative mRNA levels are shown as fold-changes of those of control wild-type mice. Data are expressed as mean ± S.D. (n = 6 in each group). Bars are identical to those in Fig. 2A. $^{*}P < 0.05$, $^{**}P < 0.01$, $^{***}P < 0.001$, between treated and untreated mice of the same genotype.

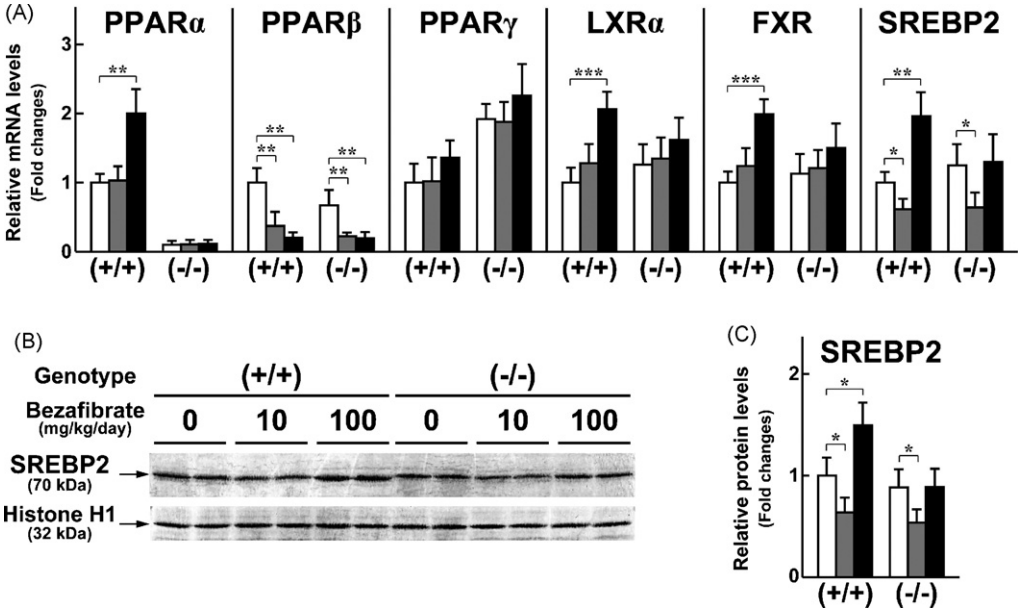

Fig. 6 – Effects of bezafibrate on transcription factor expression in wild-type (+/+) and *Ppara*-null (−/−) mice. (A) Hepatic expression of mRNA encoding transcription factors was analyzed by quantitative real-time PCR and normalized to that of GAPDH mRNA. Relative mRNA levels are shown as fold-changes of those of control wild-type mice. Data are expressed as mean ± S.D. (n = 6 in each group). Bars are identical to those in Fig. 2A. $^{*}P < 0.05$, $^{**}P < 0.01$, $^{***}P < 0.001$, between treated and untreated mice of the same genotype. (B) Immunoblot analysis of nuclear SREBP2. Hepatic nuclear fraction was prepared for each mouse, and 50 μg of protein was loaded into each well. The histone H1 band was used as the loading control. Results are representative of three independent experiments. Doses of bezafibrate are indicated above the bands of each treatment group. (C) Quantification of nuclear SREBP2 levels. Band intensity was quantified densitometrically and normalized to that of histone H1. Relative protein levels are shown as fold-changes of those of control wild-type mice. Data are expressed as mean ± S.D. (n = 6 in each group). Bars are identical to those in Fig. 2A. $^{*}P < 0.05$, between treated and untreated mice of the same genotype.

Mrp3, ABCG5, and ABCG8 in wild-type mice (Fig. 5A). No such effects from low-dose treatment were noted. Expression of bile salt export pump (BSEP) mRNA was constant.

Next, the expression of mRNA encoding bile salt transporters was examined since approximately 95% of bile salts are reabsorbed in the liver through enterohepatic circulation [29]. High-dose bezafibrate treatment significantly enhanced sodium-taurocholate cotransporting polypeptide (NTCP) mRNA expression in both genotypes, while low-dose treatment did not (Fig. 5B). Levels of organic anion transporting polypeptide 1 (OATP1) and OATP2 mRNA were unchanged by the treatment.

3.6. Alterations in transcription factor expression

In order to investigate changes in transcription factors, the expression of mRNA encoding PPARs and other factors related to cholesterol metabolism was evaluated. High-dose bezafibrate treatment markedly elevated mRNA levels of PPARα, liver X receptor α (LXRα), farnesoid X receptor (FXR), and SREBP2 in wild-type mice only (Fig. 6A). Interestingly, the low-dose treatment significantly down-regulated SREBP2 mRNA levels in both genotypes (Fig. 6A). PPARβ mRNA was considerably decreased by bezafibrate in both genotypes at both dosages, while PPARγ mRNA remained unchanged. Immunoblot analysis showed that the changes in nuclear SREBP2 levels were in accordance with those at the transcriptional levels (Fig. 6B and C). Additionally, nuclear SREBP2 levels were correlated with the expression of its target genes, such as HMGS, HMGR, FPPS, and SQS (Fig. 2).

3.7. Effects on PPAR target gene expression and peroxisome proliferation

As described above, several PPARα-independent effects were found in the low-dose bezafibrate treatment group, leading to the hypothesis that low doses of bezafibrate function via mechanisms other than PPARα activation. To address this

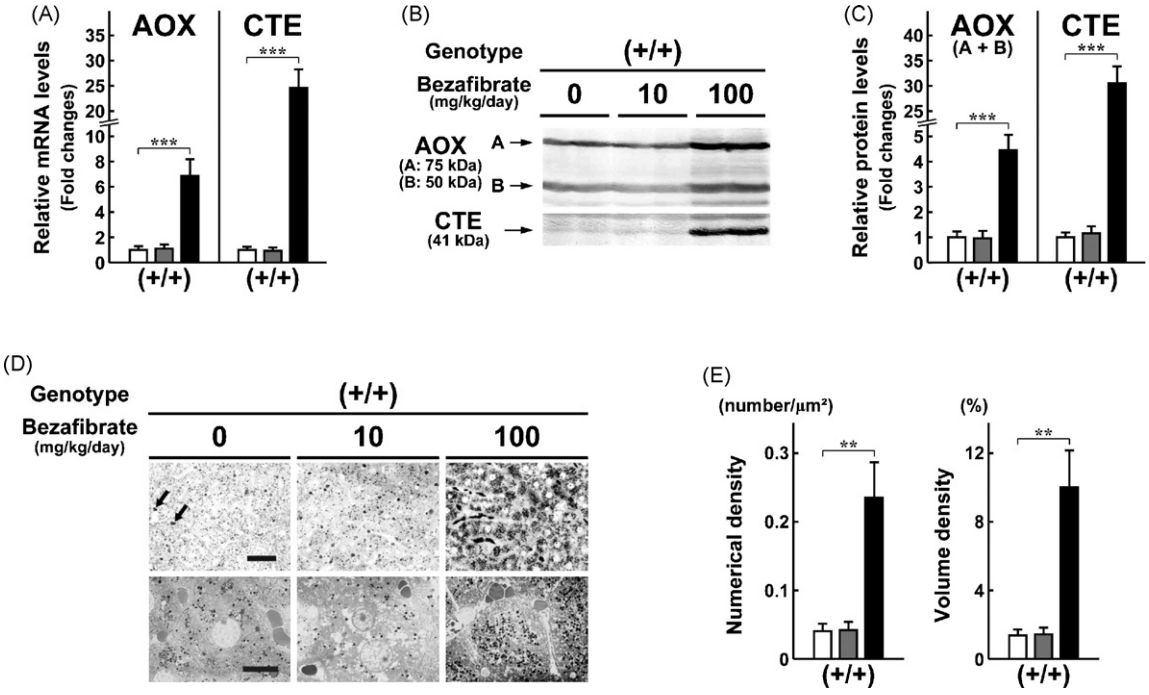

Fig. 7 – Effects of bezafibrate on PPARα target gene expression and peroxisome proliferation in wild-type (+/+) mice. (A) Hepatic expression of mRNA encoding PPARα target genes, AOX and CTE, was analyzed by quantitative real-time PCR and normalized to that of GAPDH mRNA. Relative mRNA levels are shown as fold-changes of those of control mice. Data are expressed as mean ± S.D. ($n = 6$ in each group). Bars are identical to those in Fig. 2A. ***$P < 0.001$, between treated and untreated mice. (B) Immunoblot analysis of AOX and CTE. The same samples in Fig. 2B were used. Protein sample of 50 μg was loaded into each well. Results are representative of three independent experiments. Doses of bezafibrate are indicated above the bands of each treatment group. A and B in AOX bands indicate full-length and truncated AOX, respectively. (C) Quantification of AOX and CTE protein levels. Band intensity was quantified densitometrically and normalized to that of actin. Relative protein levels are shown as fold-changes of those of control mice. Data are expressed as mean ± S.D. ($n = 6$ in each group). Bars are identical to those in Fig. 2A. ***$P < 0.001$, between treated and untreated mice. (D) Cytochemical staining of hepatic peroxisomes. Peroxisomes are detectable as dark particles, and marked peroxisome proliferation can be observed only in mice with high-dose bezafibrate treatment. The bars in the light (upper) and electron (lower) photomicrographs of control mice indicate 40 and 10 μm, respectively. The arrows indicate erythrocytes. (E) Morphometric analysis of hepatic peroxisomes. The number of peroxisomes and area of each individual peroxisomal profile were measured in ten electron photomicrographs from each mouse, and numerical and volume densities were calculated. Data are expressed as mean ± S.D. ($n = 6$ in each group). Bars are identical to those in Fig. 2A. **$P < 0.01$, between treated and untreated mice.

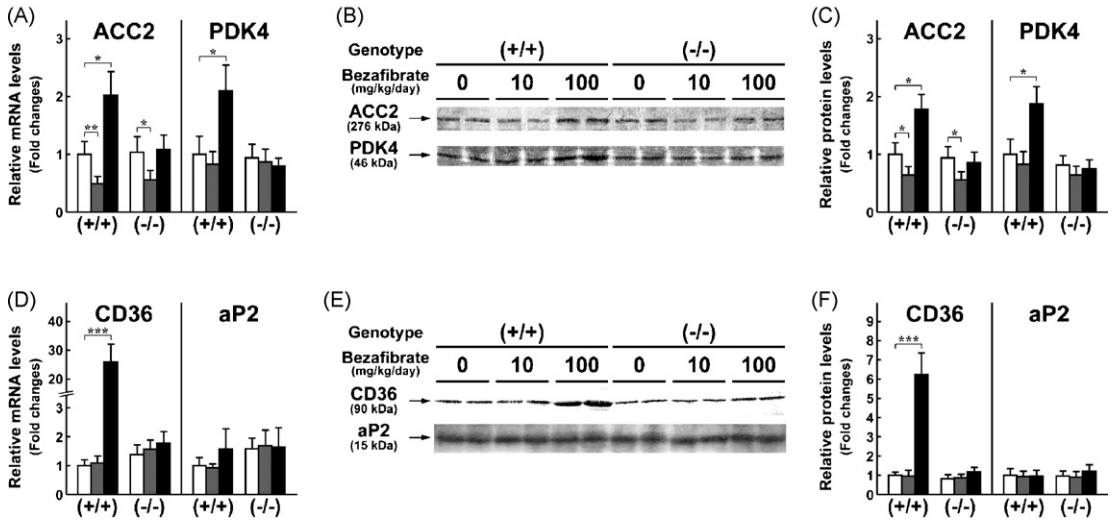

Fig. 8 – Effects of bezafibrate on PPARβ or PPARγ target gene expression in wild-type (+/+) and *Ppara*-null (−/−) mice. Hepatic expression of PPARβ target genes (ACC2 and PDK4) (A-C) and PPARγ target genes (CD36 and aP2) (D-F) was examined using quantitative real-time PCR and immunoblot analysis. The same samples in Fig. 2A and B were used. For immunoblot analysis, 50 μg of protein was loaded into each well. Data are expressed as mean ± S.D. ($n = 6$ in each group). Bars are identical to those in Fig. 2A. *$P < 0.05$, **$P < 0.01$, ***$P < 0.001$, between treated and untreated mice of the same genotype.

issue, the expression of representative PPARα target genes, including AOX and CTE [30], was investigated in wild-type mice. As expected, high-dose bezafibrate treatment markedly elevated expression of these genes, but low-dose treatment did not (Fig. 7A–C). These findings were in agreement with the result that PPARα mRNA was not elevated by low-dose administration (Fig. 6A) since PPARα activation is known to activate its own transcription [11,31]. Additionally, peroxisome proliferation, a well-known indicator of PPARα activation [22], was not observed in the low-dose group (Fig. 7D and E). Furthermore, to determine the contribution of low-dose bezafibrate on PPARβ and/or PPARγ activation, the expression of target genes of PPARβ (ACC2 [32] and PDK4 [33]), PPARα/γ (CD36 [34]), and PPARγ (aP2 [35]) were analyzed in both genotypes, but showed no increase in mice treated with low-dose bezafibrate (Fig. 8). Overall, these results strongly suggest that low doses of bezafibrate do not induce significant activation of murine PPARs.

4. Discussion

The present study provides novel and unexpected evidence that the pharmacological action of bezafibrate on cholesterol metabolism varies considerably according to its dosage. Treatment with high-dose bezafibrate (100 mg/kg/day), a dosage similar to that used in previous rodent experiments, resulted in both a slight increase in serum TC concentration and a marked decrease in hepatic TC in a PPARα-dependent manner, accompanied with strong PPAR activation. In contrast, treatment with low-dose bezafibrate (10 mg/kg/day), corresponding approximately to the dosage used in human clinical practice, decreased serum and hepatic cholesterol concentrations in the absence of significant PPAR activation. As far as we know, this is the first study that explores the dose-dependent effects of bezafibrate in mice.

High-dose bezafibrate treatment caused several conflicting changes in the mRNA levels of various enzymes, transporters, and receptors related to hepatic cholesterol metabolism in a PPARα-dependent fashion. Specifically, mRNA levels of proteins involved in cholesterol biosynthesis (HMGS, HMGR, FPPS, and SQS), catabolism (CYP7A1, CYP8B1, and AOX2), uptake (SR-B1 and LDLR), and excretion (apoA2, apoE, ABCA1, and ABCG5/8) were all elevated. Although this simultaneous induction was too complicated to interpret all of the molecular mechanisms involved, these responses were likely associated with the both direct and indirect effects of intensive PPAR activation. It is conceivable that the elevated levels of LXRα, FXR, and SREBP2 found following high-dose bezafibrate treatment affected the expression of numerous proteins involved in cholesterol/bile acid metabolism; all three have been shown to regulate expression of CYP7A1 and ABC transporters [36,37], apoE, Mdr2, and Mrp2 [38–40], and cholesterogenic enzymes and LDLR [41,42]. Moreover, hepatic expression of the xenobiotic transporter Mdr1 was up-regulated by high-dose treatment in a PPARα-dependent manner, suggesting the possible influence of PPARα activation-induced stress, such as rodent-specific hepatomegaly [13]. Therefore, previous results in rodents treated with high-dose bezafibrate may not accurately reflect the pharmacological effect of this drug in humans.

The molecular mechanism of the cholesterol-reducing effect of low-dose bezafibrate seemed to be due to suppression of SREBP2-regulated de novo cholesterogenesis and stimulation of cholesterol catabolism through increased expression of two 7α-hydroxylases, CYP7A1 and CYP7B1. A previous study suggested that the expression of human CYP7B1 is suppressed by SREBPs [43]. In the present study, CYP7B1 expression in

both genotypes under low-dose bezafibrate treatment reacted inversely to SREBP2; therefore, increases in CYP7B1 expression might be accompanied by attenuation of SREBP2. In contrast to CYP7B1, CYP7A1 expression was up-regulated by bezafibrate treatment in a PPARα-independent, dose-dependent manner. Thus, these changes might be attributable to some as yet unknown bezafibrate-specific action. The down-regulation of SREBP2 by low-dose treatment occurred at the transcriptional level. Transcription of SREBP2 is known to be regulated by mature SREBP2 translocated to the nucleus through a proteolytic processing step controlled by several proteins, including SREBP cleavage-activating protein and site-1 protease [41,42,44,45]. Bezafibrate might influence the proteolysis of SREBP2 through modulation of such factors, though further experiments are needed in this regard.

The present study revealed that low-dose bezafibrate treatment increased the expression of ABCA1, NPC1, and L-FABP in the presence of PPARα. Previous reports have established a prominent role for hepatic ABCA1 in the regulation of plasma high-density lipoprotein cholesterol levels [46,47]. In addition, NPC1 has been shown to transport free cholesterol from lysosomes to the plasma membrane, contributing to cholesterol efflux through the ABCA1 pathway [48]. Therefore, these changes may be partly related to bezafibrate enhancement of high-density lipoprotein cholesterol in humans. L-FABP is known as a major bile acid transporter [49,50], and the enhancement of its expression may be implicated in facilitation of intracellular bile acid mobility. Recently, the efficacy of bezafibrate has been demonstrated in patients with chronic cholestatic liver diseases, such as primary biliary cirrhosis [51–53]. The present results concerning L-FABP induction might partially explain the beneficial effects of bezafibrate against such diseases. Taken together, our results suggest the importance of PPARα on understanding the pharmacological effects of bezafibrate.

The above-mentioned dose discrepancy between rodents and humans could be due to pharmacokinetic differences; dose justification alone might be inadequate to compare the conditions. However, our preliminary analysis and the previous reports have demonstrated that maximum plasma concentrations (C_{max}) and area under the concentration–time curve (AUC) values in rats after the single high-dose administration of bezafibrate were quite different from those in healthy volunteers after the single intake at the clinical dose (mean C_{max}, 140 μg/mL vs. 11 μg/mL; mean AUC values, 1520 μg·h/mL vs. 39 μg·h/mL) [54,55]. On the other hand, these parameters in rats after the single low-dose administration were relatively similar to those in healthy volunteers (21 μg/mL and 107 μg·h/mL, respectively). Therefore, the phenomena observed in mice under low-dose administration might reflect the conditions in bezafibrate-treated humans more accurately than those in mice with high-dose administration.

This study showed that low-dose bezafibrate treatment reduced circulating cholesterol and altered hepatic cholesterol metabolism through a PPARα-independent mechanism in mice. Although no significant activation of any PPAR subtype was determined under low-dose treatment as estimated by the expression of various PPAR target genes and morphometry of hepatic peroxisomes, we cannot rule out the possibility that the PPARα-independent effect was nonetheless somehow mediated by PPARβ, PPARγ, or both. Further studies using mice lacking all PPAR subtypes are needed to address this issue. Additionally, cholesterol-metabolizing pathways in mice partly differ from those in humans. For example, the degree of contribution of the alternative pathway to overall bile acid synthesis is thought to be low in mice compared to humans [36]. The same experiment using other mammals such as guinea pigs, which have more similarities in cholesterol metabolism to humans than mice [56,57], would confirm our results.

In conclusion, we demonstrated that the cholesterol-reducing effect of bezafibrate in mice at the clinically-relevant dose stems from suppression of cholesterol biosynthesis and enhancement of catabolism without significant PPAR activation. Additionally, our results indicated remarkable differences in the mechanisms involved in bezafibrate action by comparing high-dose and low-dose treatments. These findings may lead to better identification of the mechanisms underlying the beneficial effects of bezafibrate in patients with dyslipidemia.

Conflicts of interest

None.

Acknowledgement

We thank Trevor Ralph for editorial assistance.

REFERENCES

[1] Schulzeck P, Bojanovski M, Jochim A, Canzler H, Bojanovski D. Comparison between simvastatin and bezafibrate in effect on plasma lipoproteins and apolipoproteins in primary hypercholesterolaemia. Lancet 1988;1:611–3.
[2] Pazzucconi F, Mannucci L, Mussoni L, Gianfranceschi G, Maderna P, Werba P, et al. Bezafibrate lowers plasma lipids, fibrinogen and platelet aggregability in hypertriglyceridaemia. Eur J Clin Pharmacol 1992;43:219–23.
[3] Bradford RH, Goldberg AC, Schonfeld G, Knopp RH. Double-blind comparison of bezafibrate versus placebo in male volunteers with hyperlipoproteinemia. Atherosclerosis 1992;92:31–40.
[4] Roglans N, Bellido A, Rodríguez C, Cabrero À, Novell F, Ros E, et al. Fibrate treatment does not modify the expression of acyl coenzyme A oxidase in human liver. Clin Pharmacol Ther 2002;72:692–701.
[5] The BIP Study Group. Secondary prevention by raising HDL cholesterol and reducing triglycerides in patients with coronary artery disease: the Bezafibrate Infarction Prevention (BIP) study. Circulation 2000;102:21–7.
[6] Staels B, Dallongeville J, Auwerx J, Schoonjans K, Leitersdorf E, Fruchart JC. Mechanism of action of fibrates on lipid and lipoprotein metabolism. Circulation 1998;98:2088–93.
[7] Desvergne B, Wahli W. Peroxisome proliferator-activated receptors: nuclear control of metabolism. Endocr Rev 1999;20:649–88.

[8] Aoyama T, Peters JM, Iritani N, Nakajima T, Furihata K, Hashimoto T, et al. Altered constitutive expression of fatty acid-metabolizing enzymes in mice lacking the peroxisome proliferator-activated receptor α (PPARα). J Biol Chem 1998;273:5678–84.
[9] Nakajima T, Kamijo Y, Tanaka N, Sugiyama E, Tanaka E, Kiyosawa K, et al. Peroxisome proliferator-activated receptor α protects against alcohol-induced liver damage. Hepatology 2004;40:972–80.
[10] Kamijo Y, Hora K, Nakajima T, Kono K, Takahashi K, Ito Y, et al. Peroxisome proliferator-activated receptor α protects against glomerulonephritis induced by long-term exposure to the plasticizer di-(2-ethylhexyl)phthalate. J Am Soc Nephrol 2007;18:176–88.
[11] Tanaka N, Moriya K, Kiyosawa K, Koike K, Gonzalez FJ, Aoyama T. PPARα activation is essential for HCV core protein-induced hepatic steatosis and hepatocellular carcinoma in mice. J Clin Invest 2008;118:683–94.
[12] Hunt MC, Yang YZ, Eggertsen G, Carneheim CM, Gåfvels M, Einarsson C, et al. The peroxisome proliferator-activated receptor α (PPARα) regulates bile acid biosynthesis. J Biol Chem 2000;275:28947–53.
[13] Kok T, Bloks VW, Wolters H, Havinga R, Jansen PLM, Staels B, et al. Peroxisome proliferator-activated receptor α (PPARα)-mediated regulation of multidrug resistance 2 (Mdr2) expression and function in mice. Biochem J 2003;369:539–47.
[14] Brown PJ, Winegar DA, Plunket KD, Moore LB, Lewis MC, Wilson JG, et al. A ureido-thioisobutyric acid (GW9578) is a subtype-selective PPARα agonist with potent lipid-lowering activity. J Med Chem 1999;42:3785–8.
[15] Inoue I, Itoh F, Aoyagi S, Tazawa S, Kusama H, Akahane M, et al. Fibrate and statin synergistically increase the transcriptional activities of PPARα/RXRα and decrease the transactivation of NFκB. Biochem Biophys Res Commun 2002;290:131–9.
[16] Peters JM, Aoyama T, Burns AM, Gonzalez FJ. Bezafibrate is a dual ligand for PPARα and PPARβ: studies using null mice. Biochim Biophys Acta 2003;1632:80–9.
[17] Poirier H, Niot I, Monnot MC, Braissant O, Meunier-durmort C, Costet P, et al. Differential involvement of peroxisome-proliferator-activated receptors α and δ in fibrate and fatty-acid-mediated inductions of the gene encoding liver fatty-acid-binding protein in the liver and the small intestine. Biochem J 2001;355:481–8.
[18] Hays T, Rusyn I, Burns AM, Kennett MJ, Ward JM, Gonzalez FJ, et al. Role of peroxisome proliferator-activated receptor-α (PPARα) in bezafibrate-induced hepatocarcinogenesis and cholestasis. Carcinogenesis 2005;26:219–27.
[19] Nagasawa T, Inada Y, Nakano S, Tamura T, Takahashi T, Maruyama K, et al. Effects of bezafibrate, PPAR pan-agonist, and GW501516, PPARδ agonist, on development of steatohepatitis in mice fed a methionine- and choline-deficient diet. Eur J Pharmacol 2006;536:182–91.
[20] Osumi T, Hashimoto T, Ui N. Purification and properties of acyl-CoA oxidase from rat liver. J Biochem 1980;87:1735–46.
[21] Miyazawa S, Furuta S, Hashimoto T. Induction of a novel long-chain acyl-CoA hydrolase in rat liver by administration of peroxisome proliferators. Eur J Biochem 1981;117:425–30.
[22] Lee SS, Pineau T, Drago J, Lee EJ, Owens JW, Kroetz DL, et al. Targeted disruption of the α isoform of the peroxisome proliferator-activated receptor gene in mice results in abolishment of the pleiotropic effects of peroxisome proliferators. Mol Cell Biol 1995;15:3012–22.
[23] Usui S, Hara Y, Hosaki S, Okazaki M. A new on-line dual enzymatic method for simultaneous quantification of cholesterol and triglycerides in lipoproteins by HPLC. J Lipid Res 2002;43:805–14.
[24] Hara A, Radin NS. Lipid extraction of tissues with a low-toxicity solvent. Anal Biochem 1978;90:420–6.
[25] Carr TP, Andresen CJ, Rudel LL. Enzymatic determination of triglyceride, free cholesterol, and total cholesterol in tissue lipid extracts. Clin Biochem 1993;26:39–42.
[26] Aoyama T, Uchida Y, Kelley RI, Marble M, Hofman K, Tonsgard JH, et al. A novel disease with deficiency of mitochondrial very-long-chain acyl-CoA dehydrogenase. Biochem Biophys Res Commun 1993;191:1369–72.
[27] Aoyama T, Souri M, Ushikubo S, Kamijo T, Yamaguchi S, Kelley RI, et al. Purification of human very-long-chain acyl-coenzyme A dehydrogenase and characterization of its deficiency in seven patients. J Clin Invest 1995;95:2465–73.
[28] Tanaka N, Moriya K, Kiyosawa K, Koike K, Aoyama T. Hepatitis C virus core protein induces spontaneous and persistent activation of peroxisome proliferator-activated receptor α in transgenic mice: implications for HCV-associated hepatocarcinogenesis. Int J Cancer 2008;122: 124–31.
[29] Trauner M, Boyer JL. Bile salt transporters: molecular characterization, function, and regulation. Physiol Rev 2003;83:633–71.
[30] Mandard S, Müller M, Kersten S. Peroxisome proliferator-activated receptor α target genes. Cell Mol Life Sci 2004;61:393–416.
[31] Tanaka N, Hora K, Makishima H, Kamijo Y, Kiyosawa K, Gonzalez FJ, et al. In vivo stabilization of nuclear retinoid X receptor α in the presence of peroxisome proliferator-activated receptor α. FEBS Lett 2003;543:120–4.
[32] Lee CH, Olson P, Hevener A, Mehl I, Chong LW, Olefsky JM, et al. PPARδ regulates glucose metabolism and insulin sensitivity. Proc Natl Acad Sci USA 2006;103:3444–9.
[33] Degenhardt T, Saramäki A, Malinen M, Rieck M, Väisänen S, Huotari A, et al. Three members of the human pyruvate dehydrogenase kinase gene family are direct targets of the peroxisome proliferator-activated receptor β/δ. J Mol Biol 2007;372:341–55.
[34] Motojima K, Passilly P, Peters JM, Gonzalez FJ, Latruffe N. Expression of putative fatty acid transporter genes are regulated by peroxisome proliferator-activated receptor α and γ activators in a tissue- and inducer-specific manner. J Biol Chem 1998;273:16710–4.
[35] Memon RA, Tecott LH, Nonogaki K, Beigneux A, Moser AH, Grunfeld C, et al. Up-regulation of peroxisome proliferator-activated receptors (PPAR-α) and PPAR-γ messenger ribonucleic acid expression in the liver in murine obesity: troglitazone induces expression of PPAR-γ-responsive adipose tissue-specific genes in the liver of obese diabetic mice. Endocrinology 2000;141:4021–31.
[36] Chiang JYL. Bile acid regulation of gene expression: roles of nuclear hormone receptors. Endocr Rev 2002;23:443–63.
[37] Kok T, Wolters H, Bloks VW, Havinga R, Jansen PLM, Staels B, et al. Induction of hepatic ABC transporter expression is part of the PPARα-mediated fasting response in the mouse. Gastroenterology 2003;124:160–71.
[38] Mak PA, Kast-Woelbern HR, Anisfeld AM, Edwards PA. Identification of PLTP as an LXR target gene and apoE as an FXR target gene reveals overlapping targets for the two nuclear receptors. J Lipid Res 2002;43:2037–41.
[39] Moschetta A, Bookout AL, Mangelsdorf DJ. Prevention of cholesterol gallstone disease by FXR agonists in a mouse model. Nat Med 2004;10:1352–8.
[40] Claudel T, Staels B, Kuipers F. The farnesoid X receptor: a molecular link between bile acid and lipid and glucose metabolism. Arterioscler Thromb Vasc Biol 2005;25: 2020–30.
[41] Brown MS, Goldstein JL. The SREBP pathway: regulation of cholesterol metabolism by proteolysis of a membrane-bound transcription factor. Cell 1997;89:331–40.

[42] Horton JD, Goldstein JL, Brown MS. SREBPs: activators of the complete program of cholesterol and fatty acid synthesis in the liver. J Clin Invest 2002;109:1125–31.
[43] Norlin M, Chiang JYL. Transcriptional regulation of human oxysterol 7α-hydroxylase by sterol response element binding protein. Biochem Biophys Res Commun 2004;316:158–64.
[44] Matsuda M, Korn BS, Hammer RE, Moon YA, Komuro R, Horton JD, et al. SREBP cleavage-activating protein (SCAP) is required for increased lipid synthesis in liver induced by cholesterol deprivation and insulin elevation. Genes Dev 2001;15:1206–16.
[45] Yang J, Goldstein JL, Hammer RE, Moon YA, Brown MS, Horton JD. Decreased lipid synthesis in livers of mice with disrupted Site-1 protease gene. Proc Natl Acad Sci USA 2001;98:13607–12.
[46] Basso F, Freeman L, Knapper CL, Remaley A, Stonik J, Neufeld EB, et al. Role of the hepatic ABCA1 transporter in modulating intrahepatic cholesterol and plasma HDL cholesterol concentrations. J Lipid Res 2003;44:296–302.
[47] Ragozin S, Niemeier A, Laatsch A, Loeffler B, Merkel M, Beisiegel U, et al. Knockdown of hepatic ABCA1 by RNA interference decreases plasma HDL cholesterol levels and influences postprandial lipemia in mice. Arterioscler Thromb Vasc Biol 2005;25:1433–8.
[48] Chinetti-Gbaguidi G, Rigamonti E, Helin L, Mutka AL, Lepore M, Fruchart JC, et al. Peroxisome proliferator-activated receptor α controls cellular cholesterol trafficking in macrophages. J Lipid Res 2005;46:2717–25.
[49] Thumser AEA, Wilton DC. The binding of cholesterol and bile salts to recombinant rat liver fatty acid-binding protein. Biochem J 1996;320:729–33.
[50] Martin GG, Atshaves BP, McIntosh AL, Mackie JT, Kier AB, Schroeder F. Liver fatty-acid-binding protein (L-FABP) gene ablation alters liver bile acid metabolism in male mice. Biochem J 2005;391:549–60.
[51] Kurihara T, Niimi A, Maeda A, Shigemoto M, Yamashita K. Bezafibrate in the treatment of primary biliary cirrhosis: comparison with ursodeoxycholic acid. Am J Gastroenterol 2000;95:2990–2.
[52] Kurihara T, Maeda A, Shigemoto M, Yamashita K, Hashimoto E. Investigation into the efficacy of bezafibrate against primary biliary cirrhosis, with histological references from cases receiving long term monotherapy. Am J Gastroenterol 2002;97:212–4.
[53] Kaplan MM, Gershwin ME. Primary biliary cirrhosis. N Engl J Med 2005;353:1261–73.
[54] Abshagen U, Bablok W, Koch K, Lang PD, Schmidt HAE, Senn M, et al. Disposition pharmacokinetics of bezafibrate in man. Eur J Clin Pharmacol 1979;16:31–8.
[55] Monk JP, Todd PA. Bezafibrate A review of its pharmacodynamic and pharmacokinetic properties, and therapeutic use in hyperlipidaemia. Drugs 1987;33:539–76.
[56] West KL, Fernandez ML. Guinea pigs as models to study the hypocholesterolemic effects of drugs. Cardiovasc Drug Rev 2004;22:55–70.
[57] Fernandez ML. Guinea pigs as models for cholesterol and lipoprotein metabolism. J Nutr 2001;131:10–20.